Shape, width, and replicas of π bands of single-layer graphene grown on Si-terminated vicinal SiC(0001)

Kan Nakatsuji,* Yuki Shibata, Ryota Niikura, and Fumio Komori†
Institute for Solid State Physics, University of Tokyo, 5-1-5 Kashiwanoha, Kashiwa-shi, Chiba 277-8581, Japan

Kouhei Morita and Satoru Tanaka
Department of Applied Quantum Physics and Nuclear Engineering, Kyushu University, Fukuoka 819-0395, Japan
(Received 1 March 2010; revised manuscript received 23 June 2010; published 26 July 2010)

Massless π bands of graphene grown on a SiC(0001) substrate can be affected by the scattering at the boundaries and the interface superstructure. We investigated the π band structure and width of the single- and double-layer graphenes grown on a vicinal SiC(0001) substrate using angle-resolved photoemission spectroscopy. The π electron scattering at the substrate steps makes the spectrum width anisotropic but no difference occurs in the π band shape. Quasi-2×2 replicas of the π band due to the interface $6\sqrt{3}\times6\sqrt{3}R30°$ superstructure were observed in the single-layer graphene while they were absent in the double-layer graphene.

DOI: 10.1103/PhysRevB.82.045428 PACS number(s): 73.22.Pr, 79.60.Jv

I. INTRODUCTION

Single- and few-layer graphenes have attracted much attention because of their unique electronic properties related to the massless Dirac electron features. A novel quantum-Hall effect, for example, was theoretically predicted,[1] and observed in mechanically cleaved single-layer graphenes.[2,3] For detailed measurements of their electronic properties as well as possible applications of their electronic conduction, macroscopic-scale epitaxial graphenes made on substrates have been studied experimentally by several methods. However, the presence of the substrate generally modifies the graphene electronic properties and thus it is important to study interaction between the graphene and the substrate.

One of the controversial issues on the epitaxial graphene grown on Si-terminated surface of SiC(0001),[4] where much knowledge has been accumulated so far, is the π band structure around the Dirac point E_D studied by the angle-resolved photoelectron spectroscopy (ARPES).[5,6] Interestingly, the observed π band of the single-layer graphene was not so straight around E_D as expected for an ideal graphene. This has been interpreted as consequences of the interaction of the Dirac electrons with the other degrees of freedom such as plasmon[5,7] and/or the symmetry breaking of the graphene A and B sublattices due to the interface structure.[6] In theoretical studies, the interaction with plasmon and phonons as well as the electron-hole excitation were actually assigned as the origins of the observed spectrum width of the momentum distribution curve (MDC).[7,8] Presence of these many-body effects has been recently supported by tunneling spectroscopy.[9] Whereas, the observed band dispersion was reproduced without the contributions from many-body effects when the electronic potential due to the interface $6\sqrt{3}\times6\sqrt{3}R30°$ structure of carbon atoms was theoretically considered for a single-layer graphene.[10] This superstructure gives a 13×13 potential for the graphene lattice, and a local 2×2 potential,[11] which can break the A and B sublattice symmetries.

In the present ARPES study, we use single-layer graphene grown on a vicinal SiC(0001) substrate and focus on the effect of the interface structure on the π band structure around E_D. This graphene is homogeneous with very few defects because of its step-flow growth mode[12] and the number of graphene layers can be well controlled in a millimeter scale. Moreover, the anisotropic distribution of the substrate steps enables us to study the effect of the boundary scatterings on the spectrum width and the π band shape. The steps actually affect the width while the band shape is independent of it. Replicas of the π bands at 5/13 and 8/13 of the graphene lattice due to the interface $6\sqrt{3}\times6\sqrt{3}R30°$ carbon structure are simultaneously detected for the single-layer graphene in contrast to their absence in the double-layer graphene. These replicas suggest the electronic potential modulation at the graphene layer. The results will be discussed using the recent theoretical studies on the interface structure.[10,11]

II. EXPERIMENTAL

In the experiment, single- and double-layer graphenes were grown on Si-terminated surface of vicinal nitrogen-doped 6H-SiC(0001) substrates that are commercially available. The substrates were tilted toward the $[11\bar{2}0]$ (4° off) direction. The details of the preparation and the characterization of the graphene layers were previously given.[12] Briefly, the substrate surface was first etched under atmospheric pressure of H_2 gas at 1610 K for 30 min, and a SiON film[13] was successively formed on the surface by annealing under the same pressure of N_2 gas at 1610 K for 15 min. Finally, graphene layer was made on this substrate by annealing in an ultrahigh vacuum (UHV) or N_2 gas over 1900 K for up to a few hundred seconds. The average thickness of the graphene can be controlled by the annealing temperature and time.

The surface morphology was observed by atomic force microscopy (AFM, Nanoscope IIIa, DI) at room temperature (RT) in air with topographic and phase images of the amplitude-modulation mode. The distribution of single- and double-layer graphenes was confirmed by the phase images and by low-energy electron microscopy (LEEM) in UHV at RT.[14,15] The band structure was studied using ARPES.[16] We detected photoelectrons from 3 mmϕ area of the sample at

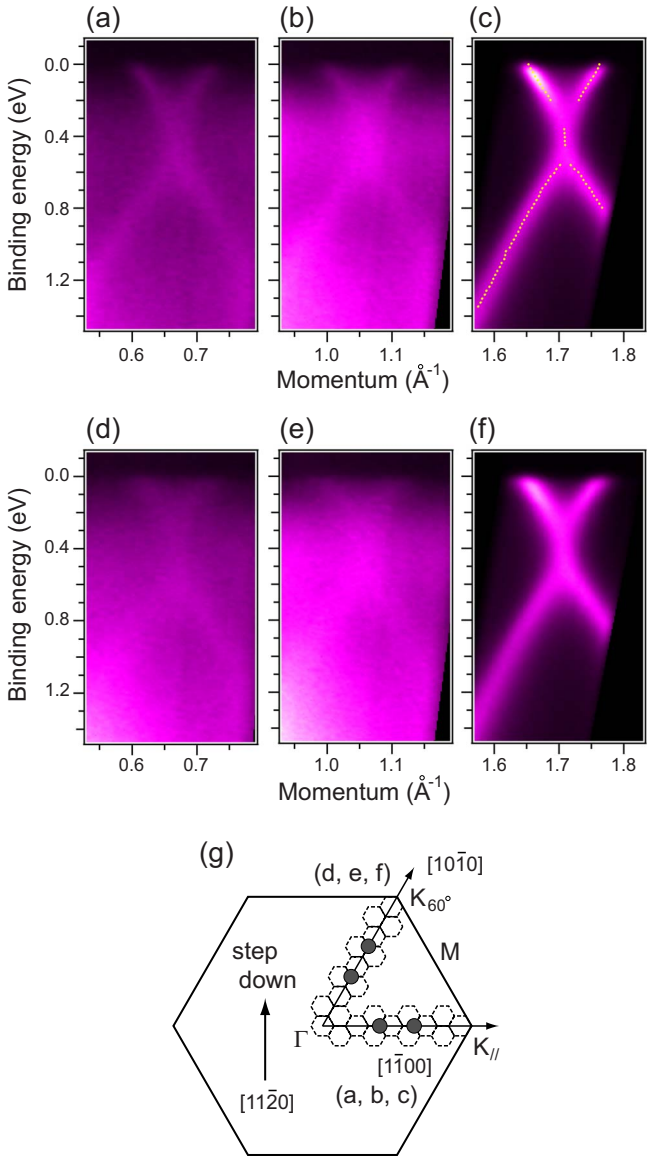

FIG. 1. (Color online) [(a)–(f)] ARPE spectra in the [1$\bar{1}$00] [(a)–(c)] and [10$\bar{1}$0] [(d)–(f)] directions for a sample with single-layer graphene. At K in the both directions, $K_{\parallel}$ (c) and $K_{60°}$ (f), the π band was clearly observed. Dotted curve in (c) indicates the spectrum peaks in MDC. At k=0.66 [(a) and (d)] and 1.06 [(b) and (e)] Å^{-1}, replicas of the π band were observed in the both directions. (g) Schematic illustration showing the step-down direction, the graphene Brillouin zone (solid hexagon), the 13×13 Brillouin zone (dotted hexagon), and the positions of the observed replicas (solid circles).

130 K by He I radiation. Before each measurement in UHV, the sample was annealed at 900 K for 30 min in UHV, and the graphene and interface $6\sqrt{3}\times6\sqrt{3}R30°$ structures were confirmed by low-energy electron diffraction (LEED).

III. RESULTS AND DISCUSSION

Figures 1(a)–1(f) show the results of the ARPES for the single-layer graphene. Here, we measured the spectra in the two directions of the substrate lattice [see Fig. 1(g)]; [1$\bar{1}$00], which is perpendicular to the step-down direction of the substrate, and [10$\bar{1}$0] directions both along the Γ-K-M lines. In the present paper, we call the K point in the [1$\bar{1}$00] direction, $K_{\parallel}$, and in the [10$\bar{1}$0] direction, $K_{60°}$. The surface morphology observed in an AFM topographic image is shown in Fig. 2(a). The terrace elongated in the [1$\bar{1}$00] direction.

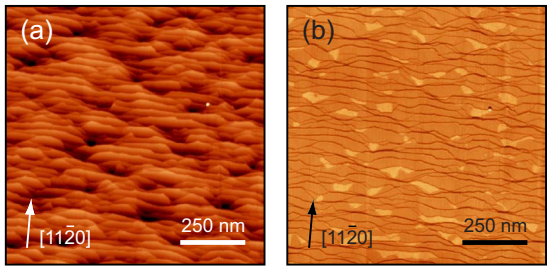

FIG. 2. (Color online) (a) AFM topographic and (b) phase-contrast images of the same area of the graphene sample. These images were obtained before the ARPES measurements shown in Figs. 1. In (b), the surface without graphene is imaged brighter than the areas covered by single-layer graphene. The dark wavy lines in (b) are steps on the surface and perpendicular to the [11$\bar{2}$0] direction on average.

The π bands at $K_{\parallel}$ and $K_{60°}$ in the reciprocal space were clearly observed in Figs. 1(c) and 1(f). They are nonlinear as indicated by the dotted curve showing the spectrum peaks of MDC in Fig. 1(c). Replicas of the π bands were seen at k =1.06 and 0.66 Å^{-1} for the both directions as in Figs. 1(a), 1(b), 1(d), and 1(e). Intensity of the replica in the [1$\bar{1}$00] direction is stronger than [10$\bar{1}$0]. No other π-band replica was detected in the Γ-$K_{\parallel}$-M and Γ-$K_{60°}$-M directions.

An AFM phase image shown in Fig. 2(b) illustrates two kinds of flat surface on the terrace; minor bright and major dark areas. Using the phase image, we can distinguish the single layer from the double layer and from the $6\sqrt{3}\times6\sqrt{3}R30°$ surface.[15] The major surface should be a single-layer graphene, which continues across the steps of the SiC substrate and is curved there.[17] We assign the minor surface as the $6\sqrt{3}\times6\sqrt{3}R30°$ surface on the basis of the LEEM and ARPES results. The LEEM observation after the AFM measurements confirmed the absence of the double layer at this surface. In ARPES measurements, no π bands from double-layer graphene at K were detected consistently.

We obtained the MDC width of the π band spectrum by fitting the data with Voigt function which is the convolution of Lorentzian and Gaussian functions. The Gaussian width is determined experimentally by the energy and momentum resolutions, and fixed at 0.0208 Å^{-1} in the fitting procedure.[18] In Fig. 3(a), the Lorentzian widths are plotted as a function of the binding energy E_B from the Fermi level. Typical MDCs are shown in Figs. 3(b) and 3(c). Parts of the widths could not be quantitatively fixed by the fitting procedure because of the band crossing at K. The results for $K_{\parallel}$ is consistent with the previous ones for the graphene with few defects on a flat surface,[5,7] where the line width was ascribed to the many-body effects. The width for the $K_{60°}$ is larger than that for the $K_{\parallel}$ in the energy region of the phonon scattering, i.e., $0<E_B<0.2$ eV while there is no significant dif-

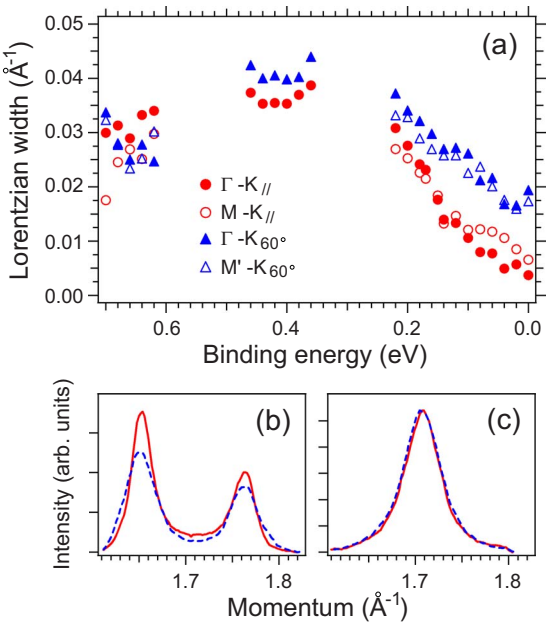

FIG. 3. (Color online) (a) Lorentzian linewidths of the π band spectra around K in the $[1\bar{1}00]$ ($K_{\parallel}$) and the $[10\bar{1}0]$ ($K_{60°}$) directions. [(b) and (c)] MDCs at (b) E_B=0.0 eV and (c) 0.4 eV. Solid and dashed curves are for $K_{\parallel}$ and $K_{60°}$.

ference in the widths of the two spectra in the other energy region.

The MDC width is determined by the elastic and inelastic scatterings that change the π electron momentum. On the terrace, the scattering rate of π electrons is expected to be isotropic. There are two kinds of the extra π electron scattering in the present graphene, those at the curved area on the substrate step edge and at the boundaries to the $6\sqrt{3}\times 6\sqrt{3}R30°$ surface. By considering the anisotropic morphology of the present single-layer graphene shown in Fig. 2, the observed anisotropy of the MDC linewidth is attributed to the scattering at the curved area. The terrace width of the graphene is typically 150 nm in the $[1\bar{1}00]$ direction, and 25 nm in the $[11\bar{2}0]$ (step-down) direction as in Fig. 2. The π electron at $K_{\parallel}$ propagates in the former direction, and that at $K_{60°}$ in the $[10\bar{1}0]$ direction, 30° rotated from the step-down direction. Consequently, the π electron at $K_{60°}$ is more frequently scattered at the curved area where its momentum changes than that at $K_{\parallel}$. This makes the MDC line width for $K_{60°}$ wider. The boundary scattering to the $6\sqrt{3}\times 6\sqrt{3}R30°$ surface could not induce the anisotropy of the MDC linewidth because the $6\sqrt{3}\times 6\sqrt{3}R30°$ is isotropically distributed. This would induce an isotropic broadening of the MDC linewidth.

The anisotropy of the scattering lifetime at Fermi energy causes anisotropic electrical transport in the graphene layers. Recent measurements of electronic conduction for the single- and double-layer graphenes on a vicinal SiC(0001) substrate[19] indicate anisotropic π electron transport due to the curved graphene at the step edges of the substrate. The resistance is smaller in the direction parallel to the step edge than that in the perpendicular direction consistently with the present ARPES result. The radius of the graphene curvature at the substrate step edges is a few nanometers and the π electrons can propagate in this area as in the carbon nanotubes while the momentum is changed at this area. Thus, the resistance in the direction perpendicular to the substrate step edge increases but remains finite.

In the present study, the anisotropy was observed only in the energy region of the phonon scattering, where the scattering rate is smaller than those at the other energy regions. Even in the phonon-scattering region, the anisotropy decreases with decreasing the electron energy from Fermi energy, i.e., increasing the intrinsic phonon-scattering rate. When these scattering rates are high on the terrace, the π electron is scattered before reaching the curved area. Thus, the scattering at the curved area less affects the total width of the MDC. The observed absence of the anisotropy means that the scattering rates due to the plasmon and electron-hole excitation on the terrace are higher than the rate due to the curved area.

In contrast to the difference in the linewidth, the observed band shape has little anisotropy as in Figs. 1(c) and 1(f), and is independent of the scattering of the π electrons at the curved areas of graphene. In a previous study,[20] the band shape changes with changing the linewidth and depends on the sample preparation condition. This result is attributed to the differences of the terrace width or the density of scattering centers for the π electron.[21] While the latter generally affects the band shape of disordered graphenes, the present single-layer graphene have a common band shape in the both directions. Thus, the nonlinear dispersion observed in the present sample must be caused by the many-body effects and/or by the interaction between the graphene layer and the interface $6\sqrt{3}\times 6\sqrt{3}R30°$ structure.

Kim *et al.*[10] and Varchon *et al.*[11] theoretically showed $6\sqrt{3}\times 6\sqrt{3}R30°$ charge density modulation at the interface carbon layer. This can modify the initial and/or final states of the photoemission process with a 13×13 lattice periodicity for the graphene layer and induce replicas of the π bands in ARPES. The 5/13 and 8/13 periodicities were found in the calculated charge density image of the interface layer.[11] This originates from a strong and local quasi-2×2 charge modulation due to the bonding between the part of C atoms in the interface layer and the Si atoms in the lower SiC layer. Experimentally, the same modulations with 5/13 and 8/13 periodicities were found in a Fourier-transformed STM image for a single-layer graphene on SiC(0001).[11]

The positions of the observed Dirac-point replicas in the Γ-K direction correspond to the 5/13 and 8/13 of the 1×1 unit vector from Γ, and are at the K points of the Brillouin zone for the 13×13 superstructure as in Fig. 1(g). The observed replicas can be, thus, attributed to the electric potential induced by the charge modulation of the interface layer. The line widths of the 5/13 and 8/13 replicas are identical to those of the corresponding original π bands within the experimental accuracy at least $0<E_B<0.1$ eV for Figs. 1(a), 1(b), 1(d), and 1(e). This is quite in contrast to the previously observed replicas[5–7] at 25 K around K points with the separation of 3/13 of the unit vector. According to Ref. 7, their width became much larger at 100 K than at 25 K. This replica was attributed to final-state diffraction because of the large difference of the spectra width between the 3/13 replica

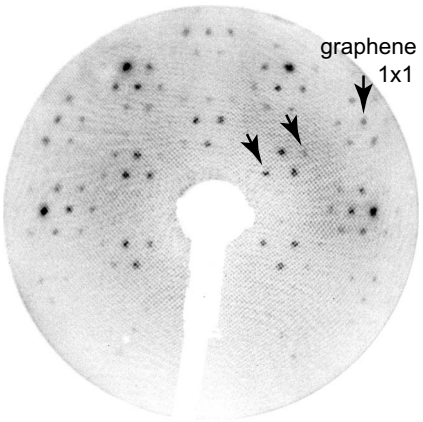

FIG. 4. LEED pattern for the present sample with single-layer graphene at the electron energy of 89 eV. The 5/13 and 8/13 spots are indicated by arrows.

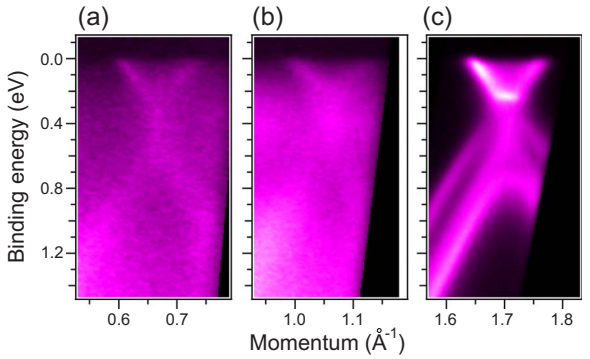

FIG. 5. (Color online) [(a)–(c)] ARPE spectra in the Γ-$K_{\parallel}$-M([$1\bar{1}00$]) direction for a sample with both single- and double-layer graphenes. The π bands for single- and double-layer graphenes are overlapped around K (c) while the replicas only for the single-layer graphene were detected at (a) k=0.66 and (b) 1.06 Å^{-1}.

and the original π band. On the other hand, the same width for the 5/13 and 8/13 replicas can support the initial-state origin. The 3/13 replica signal of a large line width could not be detected in our observation at 130 K. Difference of the photon energy between our measurements and the previous ones[5–7] may also affect the detection of the 3/13 replica because the final-state diffraction depends on the final-state electron energy.

The quasi-2×2 charge modulation in the interface carbon layer is accompanied with the lattice distortion of the same periodicity. The lattice modulations of 5/13 and 8/13 periodicities were detected in the LEED pattern of the present sample as shown in Fig. 4. The same spots were previously reported in the LEED pattern for a single-layer graphene on a flat SiC(0001) substrate.[4] However, in the calculation,[11] such a short range lattice distortion of the graphene on the interface layer was absent. The observed LEED spots of 5/13 and 8/13 are mainly due to the interface carbon layer, and the *A* and *B* sublattice asymmetry itself is not evident. Further quantitative study is necessary to understand the effect of the charge modulation in the interface layer on the adjacent graphene layer.

The replicas of the π bands at the same positions as those shown in Fig. 1 were observed for a sample with both single- and double-layer graphenes coexisting on the vicinal SiC substrate. Figures 5(a)–5(c) show results of the ARPES measurements in the Γ-$K_{\parallel}$-M direction. The replica bands were detected only from the single-layer graphene while the π bands from the both kinds of graphenes were seen at K. The LEEM observation confirmed that the fraction of the single-layer graphene is 25%.

The missing replica for the double-layer graphene indicates that the potential from the interface carbon layer is weaker for the adjacent graphene layer of the double-layer graphene than for the single-layer graphene on the same substrate. Presence of the second graphene layer alters the interface coupling between the interface carbon layer and the graphene layer. It is well known[7] that the π-band doping level of the single-layer graphene is larger than that of the interface layer of the double-layer graphene. This was evidenced by the difference of the π band shift as shown in Fig. 5(c). Consequently, the electric coupling at the interface is weak for the double layer graphene and the local potential due to the interface carbon layer for the π electrons at the adjacent graphene layer can be small. The change in the electronic structure of the interface graphene layer with increasing the layer number was previously claimed in an ARPES study.[22]

IV. CONCLUSIONS

We have investigated π bands in the Γ-$K_{\parallel}$ and Γ-K_{60° directions for the single-layer graphene grown on the vicinal SiC(0001) substrate by ARPES. The spectrum in the direction perpendicular to the step-down direction has a narrower width in the momentum distribution than the band in the other direction for $0\ \text{eV}<E_B<0.2\ \text{eV}$. Whereas, there is no significant difference in the band shape between them. The anisotropy of the linewidth is attributed to the π electron scattering at the curved areas on the substrate step edges. The origin of the observed nonlinear dispersion is not due to the π electron scatterings at the boundaries to the $6\sqrt{3}\times6\sqrt{3}R30^\circ$ surface nor at the curved area of the graphene.

The π-band replicas were observed at 5/13 and 8/13 of the 1×1 Γ-K unit vector only for the single-layer graphene. This is caused by the electrical potential due to the local quasi-2×2 charge modulation at the interface carbon layer just below the graphene layer. The same charge modulation, however, does not induce replicas in the double-layer graphene.

ACKNOWLEDGMENTS

The authors thank H. Hibino for the collaboration of the LEEM study and information of their AFM results prior to the publication. We also thank H. Kageshima for fruitful discussion on the electronic properties of few-layer graphenes. This work is partially supported by Grant-in-Aid for Scientific Research (A) under Grant No. 21244048 from the JSPS.

*nakatuji@issp.u-tokyo.ac.jp
†komori@issp.u-tokyo.ac.jp

[1] Y. Zheng and T. Ando, Phys. Rev. B **65**, 245420 (2002).
[2] K. S. Novoselov, A. K. Geim, S. V. Morozov, D. Jiang, M. I. Katsnelson, I. V. Grigorieva, S. V. Dubonos, and A. A. Firsov, Nature (London) **438**, 197 (2005).
[3] Y. Zhang, Y.-W. Tan, H. L. Störmer, and P. Kim, Nature (London) **438**, 201 (2005).
[4] J. Hass, W. A. de Heer, and E. H. Conrad, J. Phys.: Condens. Matter **20**, 323202 (2008).
[5] A. Bostwick, T. Ohta, T. Seyller, K. Horn, and E. Rotenberg, Nat. Phys. **3**, 36 (2007).
[6] S. Y. Zhou, G.-H. Gweon, A. V. Fedorov, P. N. First, W. A. de Heer, D.-H. Lee, F. Guinea, A. H. Castro Neto, and A. Lanzara, Nature Mater. **6**, 770 (2007).
[7] A. Bostwick, T. Ohta, J. L. McChesney, K. V. Emtsev, Th. Seyller, K. Horn, and E. Rotenberg, New J. Phys. **9**, 385 (2007).
[8] C.-H. Park, F. Giustino, C. D. Spataru, M. L. Cohen, and S. G. Louie, Phys. Rev. Lett. **102**, 076803 (2009).
[9] V. W. Brar, S. Wickenburg, M. Panlasigui, C.-H. Park, T. O. Wehling, Y. Zhang, R. Decker, C. Girit, A. V. Balatsky, S. G. Louie, A. Zettl, and M. F. Crommie, Phys. Rev. Lett. **104**, 036805 (2010).
[10] S. Kim, J. Ihm, H. J. Choi, and Y.-W. Son, Phys. Rev. Lett. **100**, 176802 (2008).
[11] F. Varchon, P. Mallet, J.-Y. Veuillen, and L. Magaud, Phys. Rev. B **77**, 235412 (2008).
[12] S. Tanaka, K. Morita, and H. Hibino, Phys. Rev. B **81**, 041406(R) (2010).
[13] T. Shirasawa, K. Hayashi, S. Mizuno, S. Tanaka, K. Nakatsuji, F. Komori, and H. Tochihara, Phys. Rev. Lett. **98**, 136105 (2007).
[14] H. Hibino, H. Kageshima, F. Maeda, M. Nagase, Y. Kobayashi, and H. Yamaguchi, Phys. Rev. B **77**, 075413 (2008).
[15] H. Hibino, H. Kageshima, and M. Nagase, J. Phys. D: Appl. Phys. (to be published).
[16] D. Sekiba, K. Nakatsuji, Y. Yoshimoto, and F. Komori, Phys. Rev. Lett. **94**, 016808 (2005).
[17] P. Lauffer, K. V. Emtsev, R. Graupner, Th. Seyller, L. Ley, S. A. Reshanov, and H. B. Weber, Phys. Rev. B **77**, 155426 (2008).
[18] The Gaussian width of 0.0208 $Å^{-1}$ was obtained as an average value after the fitting with Lorentzian and Gaussian width as free parameters in the energy region of Fig. 3(a). In the low binding energy region, an additional broad Gaussian was needed between the two main peaks to obtain the best fit.
[19] S. Odaka, H. Miyazaki, S.-L. Li, A. Kanda, K. Morita, S. Tanaka, Y. Miyata, H. Kataura, K. Tsukagoshi, and Y. Aoyagi, Appl. Phys. Lett. **96**, 062111 (2010).
[20] S. Y. Zhou, D. A. Siegel, A. V. Fedorov, F. El Gabaly, A. K. Schmid, A. H. Castro Neto, D.-H. Lee, and A. Lanzara, Nature Mater. **7**, 259 (2008).
[21] E. Rotenberg, A. Bostwick, T. Ohta, J. L. McChesney, T. Seyller, and K. Horn, Nature Mater. **7**, 258 (2008).
[22] A. Nagashima, H. Itoh, T. Ichinokawa, C. Oshima, and S. Otani, Phys. Rev. B **50**, 4756 (1994).